Weak signal propagation through noisy feedforward neuronal networks

Mahmut Ozer[a], Matjaž Perc[c], Muhammet Uzuntarla[a] and Etem Koklukaya[b]

We determine under which conditions the propagation of weak periodic signals through a feedforward Hodgkin–Huxley neuronal network is optimal. We find that successive neuronal layers are able to amplify weak signals introduced to the neurons forming the first layer only above a certain intensity of intrinsic noise. Furthermore, we show that as low as 4% of all possible interlayer links are sufficient for an optimal propagation of weak signals to great depths of the feedforward neuronal network, provided the signal frequency and the intensity of intrinsic noise are appropriately adjusted. ***NeuroReport*** **21:338–343 © 2010 Wolters Kluwer Health | Lippincott Williams & Wilkins.**

NeuroReport 2010, **21**:338–343

Keywords: feedforward network, Hodgkin–Huxley neurons, ion channel noise, subthreshold signal propagation

[a]Department of Electrical and Electronics Engineering, Engineering Faculty, Zonguldak Karaelmas University, Zonguldak, [b]Department of Electrical and Electronics Engineering, Engineering Faculty, Sakarya University, Sakarya, Turkey and [c]Department of Physics, Faculty of Natural Sciences and Mathematics, University of Maribor, Slovenia

Correspondence to Dr Mahmut Ozer, PhD, Department of Electrical and Electronics Engineering, Engineering Faculty, Zonguldak Karaelmas University, Zonguldak 67100, Turkey
Tel: +90 372 257 5446; fax: +90 372 257 4023;
e-mail: mahmutozer2002@yahoo.com

Received 17 November 2009 **accepted** 21 December 2009

Introduction

Complex network models have been widely used to understand how neuronal circuitry generates complex patterns of activity [1–4]. As neuronal processing often involves multiple synaptic stages, a feedforward sequence of layers of neurons has been proposed as a rudimentary platform able to shed light on how cortical circuits encode the world around us [5,6]. Within such a feedforward network, information may be encoded in different ways. In principle, information in spike trains may be encoded either through the timing of the spikes (temporal-wise) [7] or through the mean firing rate [8], indicating two possible modes of signal propagation through multiple layers. Therefore, one possible way for propagation of information in such systems is provided through the firing rate of neurons, that is, the firing-rate propagation. In this context, Shadlen and Newsome [9] studied the variable discharge of cortical neurons in a single layer with a balance between excitation and inhibition, and found that an ensemble of 100 neurons with an integrate and fire mechanism provides a reliable estimate of rate encoding within 10–50 ms long time intervals. More recently, however, it has been shown that it is difficult to transmit the firing rate of a whole population faithfully through many layers in feedforward networks with an exact balance [6], which is in contradiction with the results presented in Ref. [9]. Rossum *et al.* [10] constructed a different network architecture with multiple layers, having all-to-all connectivity, and suggested that information can be rapidly encoded by means of the firing rate of the population, and moreover, that information can propagate through many layers even with a remarkably small number of neurons per layer ($\sim$20) by adding an appropriate amount of noise to the system. In their study, noise sets the operating regimen of the network as in single layer networks. The second mode of signal propagation, as an alternative to the firing rate encoding, is temporal encoding (also termed synfire propagation), in which information is carried by a wave of synchronous activity of small groups of neurons constituting the network [11]. Recently, Reyes [12] constructed feedforward networks consisting of 10 layers, each with several hundred real cortical neurons, and showed that the firing of neurons was asynchronous in the first few layers, but became gradually more synchronous in successive layers. This experimental finding supports the notion that feedforward cortical neurons use the temporal encoding for fast and reliable signal propagation and processing [5].

Indeed, understanding the detection and propagation of weak signals in neuronal networks is of great importance. Although the subject has been widely investigated on the level of single cells [13,14] and neuronal networks with different topologies [3,4,15], it has thus far been only partly addressed for feedforward networks [16,17]. In both earlier studies [16,17], a subthreshold periodic stimulus was injected to all neurons forming the first layer of a 10-layer feedforward network in the presence of external noise, and the success of the propagation of the weak signal was investigated through the signal-to-noise ratio. It has been reported [16,17] that the signal-to-noise ratio decreases as the layer index increases, and that in a given frequency range of the stimulus the transmission is enhanced. The models investigated in Refs [16,17] considered noise as an external additive current. However, because the source of noisy activity in neuronal

 DOI: 10.1097/WNR.0b013e328336ee62

dynamics is primarily internal, an external source of noise may be biologically questionable [18]. The present work aims to further facilitate the understanding of weak signal propagation in feedforward neuronal networks. Therefore, we use a biophysically more realistic model of individual neuronal dynamics for each neuron constituting the feedforward network, where the stochastic behavior of voltage-gated ion channels embedded in neuronal membranes is modeled depending on the cell size. This allows relating the cell size to the level of intrinsic noise in a manner that more closely mimics actual conditions. In addition, the measure for the effectiveness of signal propagation, that is, information transmission, used at present is also different from what was used in Refs [16,17]. Here, we focus explicitly on the presence of a given signal frequency in the output of each layer. We thus measure explicitly the propagation of weak signals by tracking the presence of different frequencies in neuronal responses through successive layers of the feedforward network in dependence on the intensity of intrinsic noise and density of interlayer links.

Methods

We use a 10-layer feedforward neuronal network model that is conceptually similar to the one used earlier in Refs [16,17], where each individual layer consists of $L = 200$ Hodgkin–Huxley (HH) neurons [19], and each neuron receives synaptic inputs from 10% (unless stated otherwise) of randomly selected neurons in the preceding layer. There are no connections among the neurons in individual layers. The time evolution of the membrane potential for the HH neurons is given by:

$$C_m \frac{dV_{i,j}}{dt} = -g_{Na} m_{i,j}^3 h_{i,j} (V_{i,j} - V_{Na}) - g_K n_{i,j}^4 (V_{i,j} - V_K) - g_L (V_{i,j} - V_L) - I_{i,j}^{syn}(t) \quad (1)$$

where $V_{i,j}$ denotes the membrane potential of the j-th neuron in layer i ($i = 1,2,\ldots,10$ and $j = 1,2,\ldots,200 = L$). The membrane capacity is $C_m = 1\,\mu F/cm^2$, whereas $g_{Na} = 120\,mS/cm^2$ and $g_K = 36\,mS/cm^2$ are the maximal sodium and potassium conductances, respectively. The leakage conductance is assumed to be constant, equaling $g_L = 0.3\,mS/cm^2$, and $V_{Na} = 50\,mV$, $V_K = -77\,mV$ and $V_L = -54.4\,mV$ are the reversal potentials for the sodium, potassium, and leakage channels, respectively. The synaptic current $I_{i,j}^{syn}(t)$ is given by:

$$I_{i,j}^{syn}(t) = \frac{1}{N_{i,j}} \sum_{p=1}^{N} g_{syn} \alpha[t - t_{(i-1)p}] (V_{i,j} - V_{syn}) \quad (2)$$

with $\alpha[t] = (t/\tau)e^{-t/\tau}$. $N_{i,j}$ and $t_{(i-1)p}$ are the number of neurons in layer $i-1$ coupled to the j-th neuron in layer i and the firing time of the p-th neuron in layer $i-1$, respectively. The firing time is defined by the upward crossing of the membrane potential past a detection threshold of 0 mV, whereby the rising time of the synaptic input is assumed to be $\tau = 2$ ms. The synaptic weight is $g_{syn} = 0.6$, and V_{syn} represents the synaptic reversal potential, which is set to 0 mV, indicating that all the couplings in the network are excitatory. Finally, $m_{i,j}$ and $h_{i,j}$ denote activation and inactivation variables for the sodium channel of j-th neuron in layer i, respectively, and the potassium channel includes an activation variable $n_{i,j}$.

The effects of the channel noise can be modeled by using different computational algorithms. In this study, we use the algorithm presented by Fox [20]. In the Fox's algorithm, variables of stochastic gating dynamics are described via the Langevin generalization [20]:

$$\frac{dx_{i,j}}{dt} = \alpha_x(V_{i,j})(1 - x_{i,j}) - \beta_x(V_{i,j})x_{i,j} + \xi x_{i,j}(t),\ x_{i,j} = m_{i,j}, n_{i,j}, h_{i,j} \quad (3)$$

where $\alpha_x(V_{i,j})$ and $\beta_x(V_{i,j})$ are rate functions for the gating variable $x_{i,j}$. The probabilistic nature of the channels appears as a source of noise $\xi_{x_i,j}(t)$ in Eq. (3), which is an independent zero mean Gaussian white noise whose autocorrelation function is given by [20].

$$\langle \xi_m(t)\xi_m(t') \rangle = \frac{2\alpha_m\beta_m}{N_{Na}(\alpha_m + \beta_m)} \delta(t - t') \quad (4)$$

$$\langle \xi_h(t)\xi_h(t') \rangle = \frac{2\alpha_h\beta h}{N_{Na}(\alpha_h + \beta_h)} \delta(t - t') \quad (5)$$

$$\langle \xi_n(t)\xi_n(t') \rangle = \frac{2\alpha_n\beta_n}{N_K(\alpha_n + \beta_n)} \delta(t - t') \quad (6)$$

where N_{Na} and N_K denote the total number of sodium and potassium channels, respectively. The channel numbers are calculated as $N_{Na} = \rho_{Na}S$ and $N_K = \rho_K S$, where $\rho_{Na} = 60\,\mu m^{-2}$ and $\rho_K = 18\,\mu m^{-2}$ are the sodium and potassium channel densities, respectively. Equations (1)–(6) constitute the stochastic HH network model, where the cell size S determines the intensity of intrinsic noise. When the cell size is large enough, stochastic effects of the channel noise are negligible, and thus the stochastic model approaches the deterministic description.

Weak rhythmic activity is introduced to each neuron (unless stated otherwise) in the first layer ($i = 1$) in form of a weak, i.e. subthreshold, periodic signal $I(t) = A\sin(\omega t)$. Here A denotes the amplitude of the sinusoidal forcing current, which we set to $1.0\,\mu A/cm^2$, whereas $\omega = 2\pi/t_r$ is the corresponding angular frequency.

For each set of S and ω the temporal output of each neuron j in each of the 10 layers given by $V_{i,j}(t)$ is recorded for $T = 1000$ periods of the weak forcing, and then the collective temporal behavior of each layer is measured by averaging the membrane potential over all the neurons in

the corresponding layer $V_{i,\mathrm{avg}}(t) = L^{-1}\sum_{j=1..L} V_{i,j}(t)$ corresponding to the mean field of a random network. The correlation of each series with the frequency of the weak forcing is computed via the Fourier coefficients $Q_i = \sqrt{R_i^2 + S_i^2}$ according to [21]

$$R_i = \frac{2}{Tt_\mathrm{r}} \int_0^{t_\mathrm{r}T} V_{i,\mathrm{avg}}(t)\sin(\omega t)\mathrm{d}t \qquad (7)$$

$$S_i = \frac{2}{Tt_\mathrm{r}} \int_0^{t_\mathrm{r}T} V_{i,\mathrm{avg}}(t)\cos(\omega t)\mathrm{d}t \qquad (8)$$

We use the Fourier coefficients Q_i as a numerically effective measure for quantifying the quality of signal propagation, or equivalently information transmission, across all the layers of the feedforward neuronal network.

Results

In what follows, we will systemically analyze effects of different S and ω on the propagation of weak rhythmic activity across the layers of HH neurons through Q_i. First, we examine the dependence of Q_i on S for all layers with a fixed value for the angular frequency of the pacemaker equaling $\omega = 0.3$ m/s. Results are presented in Fig. 1. Evidently, Q_i increases sigmoidally with increasing cell size (or, equivalently, decreasing level of intrinsic noise) for each layer. Interestingly, each curve intersects at $S \cong 6\,\mu\mathrm{m}^2$, indicating two different modes for the propagation of weak rhythmic activity through successive layers. For the cell sizes $S < 6\,\mu\mathrm{m}^2$, Q_i decreases as the layer index i increases, which may result in the weak periodic forcing, introduced to the neurons in the first layer, being transmitted very weakly or even die out towards successive, deeper layers. This constitutes the first regime of the propagation of weak periodic forcing across the layers. However, for the cell sizes $S > 6\,\mu\mathrm{m}^2$, Q_i increases as the layer index i increases. Thus, the weak periodic signal introduced to all neurons in the first layer is being transmitted increasingly more efficient as the depth of the network increases. This constitutes the second regime of the propagation of weak periodic forcing across the layers. Finally, for larger cell sizes $S \geq 16\,\mu\mathrm{m}^2$ Q_i saturates. Importantly, the location of the intersection point with respect to S is frequency dependent in that lower as well as higher ω shift its occurrence towards $S \to 0\,\mu\mathrm{m}^2$, until at $\omega = 0.1$ m/s (lower limit) or $\omega = 0.9$ m/s (upper limit) the intersection disappears altogether (not shown). This must be attributed to the fact that the forcing frequency is then far from the optimal value (see results further below), and therefore successive layers do not amplify the input signal irrespective of the cell size, i.e. the first regime prevails across the whole span of S.

Fig. 1

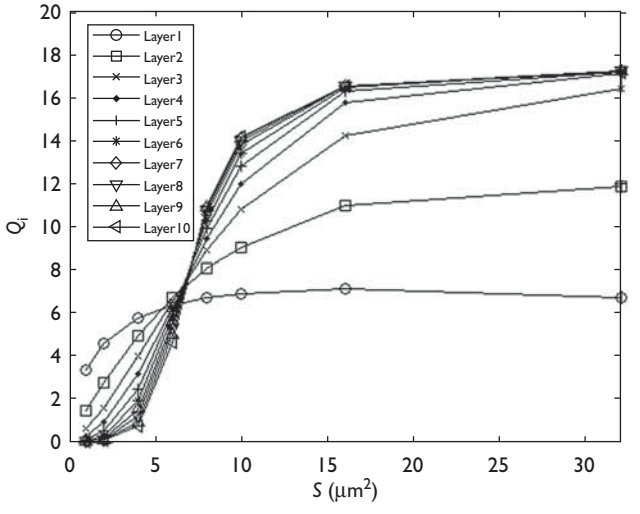

Fourier coefficients Q_i for each layer i in dependence on S with $\omega = 0.3$ m/s. Noise-supported propagation of the weak periodic forcing changes qualitatively with respect to the depth of the network at $S \cong 6\,\mu\mathrm{m}^2$ (see main text for details).

Furthermore, it is interesting to note that Q_i exhibits significant difference for the first four layers within the second regime (see e.g. symbols at $S = 10$ and $16\,\mu\mathrm{m}^2$ respectively in Fig. 1), whereas this difference gradually disappears in successive, deeper layers, suggesting that the weak periodic signal is progressively processed at deeper layers. Such a development for the outreach of the signal introduced to the first layer can be related to the experimental observations in Ref. [12] and the computational results in Refs [16,17,22], where neuronal firings in feedforward neuronal networks are asynchronous for the first layers while they become progressively more synchronous in deeper layers.

Next, we investigate how Q_i changes in dependence on the signal frequency with a fixed value of the cell size S. To that effect, we calculate the dependence of Q_i on ω for three different cell sizes. Results are presented in Fig. 2a–c for $S = 2$, 4 and $16\,\mu\mathrm{m}^2$, respectively. In agreement with results presented in Fig. 1, smaller cell sizes result in substantially lower peaks of Q_i (Fig. 2a), which increase steadily as S is enlarged (Fig. 2b and c). Interestingly, in all panels of Fig. 2, thus not depending on S, Q_i exhibits a peak at $\omega \approx 0.4$ m/s ($\cong 60$ Hz) for all i. This indicates the existence of an optimal frequency for the noise-supported propagation of weak rhythmic activity through successive layers of HH neurons. In fact, noisy HH neurons exhibit intrinsic subthreshold oscillations, giving rise to selective sensitivity to weak input signals with different frequencies. The frequency of these oscillations can be estimated through the imaginary part of the Eigen values of the corresponding steady state of an individual neuron (e.g. [23]), and the resonances with a periodic drive can thus

Fig. 2

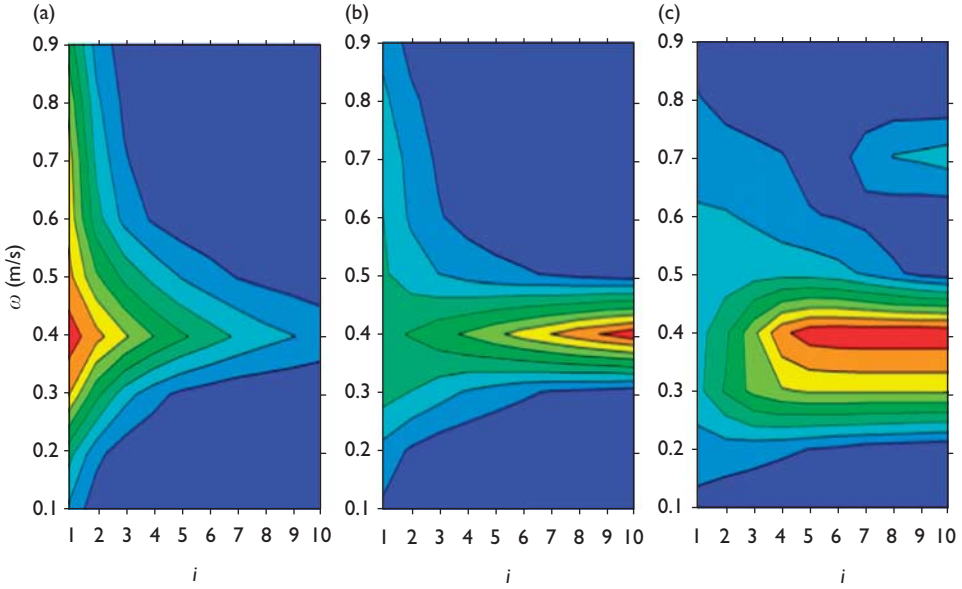

(Color online) Fourier coefficients Q_i for each layer i in dependence on ω for three different cell sizes, equaling: (a) $S=2\,\mu m^2$, (b) $S=4\,\mu m^2$ and (c) $S=16\,\mu m^2$. Note the robust existence of an optimal angular frequency $\omega \approx 0.4$ m/s($\cong 60$ Hz) irrespective of S, as well as the subsequent emergence of the secondary optimum at $\omega=0.7$ m/s, visible only for higher S [see (c)]. Color code in all panels is linear, blue depicting minimal and red maximal values of Q_i. The spans of color-coded Q_i values are (a) 0.014–5.53, (b) 0.019–14.4 and (c) 0.075–23.2.

be interpreted as an Arnold tongue. The frequency range from 30 to 80 Hz has proven most suitable for efficient encoding of weak signals that are able to optimally excite HH neurons [15–17]. The above-reported optimum of $\omega \approx 0.4$ m/s($\cong 60$ Hz) thus falls nicely within this range, especially also for networks of the small-world type [3,4], in turn explaining the existence of an optimal forcing frequency based on the individual dynamics of the HH model. These results support the fact that there exists a direct interrelation (or mapping) between oscillatory properties of individual network elements and the network rhythmicity as a whole [24]. This is also in agreement with a recent analysis, suggesting that the firing statistics of individual neurons greatly affects the behavior of the network [25].

Furthermore, when the cell size is very small, as in Fig. 2a, Q_i deteriorates with increasing i (increasing depth of the feedforward network) across the whole span of ω. However, for larger S the effect of the forcing frequency on the propagation of the weak rhythmic signal to deeper layers becomes more complex. For $S = 4\,\mu m^2$ (Fig. 2b), Q_i deteriorates with increasing i below and above the optimal forcing frequency $\omega \approx 0.4$ m/s, whereas Q_i increases with increasing i at the optimal ω. For larger cell sizes still, the frequency range for which Q_i increases with increasing i becomes broader (Fig. 2c), and interestingly covers rather exactly the most sensitive frequency range of the HH neurons (30–80 Hz) as determined by the subthreshold oscillations around the steady state. Thus, the optimal propagation of weak periodic signals towards deeper layers depends both on the cell size of neurons and the forcing frequency.

To support this argumentation further, we compute the ratio Q_{10}/Q_1 in dependence on the relevant span of S and ω, as shown in Fig. 3. By smaller S, although the optimal frequency is able to facilitate the overall transmission throughout the layers due to the resonance between the signal and the subthreshold oscillations of the HH neurons, this is not sufficient to evoke an increase in Q_i as i is becomes larger. Accordingly, the detection of the weak signal introduced at the first layer deteriorates or can even seize completely towards larger i, as evidence by $Q_{10}/Q_1 < 1$ in Fig. 3 for small S. For larger cell sizes, however, certain ranges of the forcing frequency, corresponding to the most sensitive frequency range of the HH neurons, provide the necessary ingredient enabling the switch from $Q_{10}/Q_1 < 1$ to $Q_{10}/Q_1 > 1$, thus indicating a transmission mode in which the initially weak forcing signal is increasingly amplified with the depth of the network. In Fig. 3 the amplification factor for intermediate cell sizes reaches $Q_{10}/Q_1 \approx 3$, provided the optimal $\omega \approx 0.4$ m/s is used. For even larger S the amplification factor increases further only marginally, yet the frequency range of the input signal ensuring $Q_{10}/Q_1 > 1$ broadens substantially.

Thus far, each neuron randomly received synaptic inputs from 10% of neurons in the preceding layer. In layered networks the common inputs tend to fire spikes in a

Fig. 3

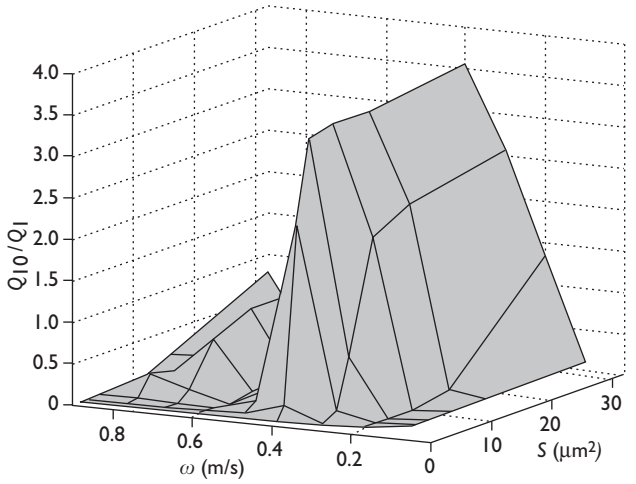

The ratio Q_{10}/Q_1 in dependence on S and ω. Results confirm the existence of an optimal forcing frequency for an efficient signal propagation through noisy feedforward neuronal networks, equaling $\omega \approx 0.4$ m/s($\cong$60 Hz), as well as the emergence of a weak secondary optimum at $\omega = 0.7$ m/s, which becomes visible only for higher S.

Fig. 4

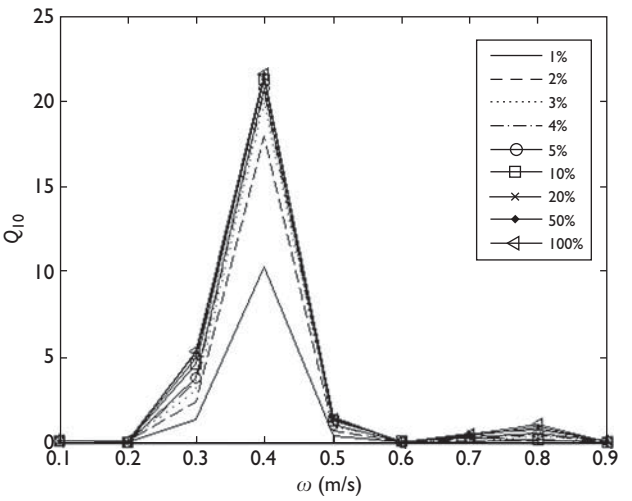

Fourier coefficient Q_{10} in dependence on ω for different densities of interlayer links. The cell size is $S = 6\,\mu m^2$. As low as 4% of all possible interlayer links guarantee optimal propagation of weak rhythmic signals through all the layers of a noisy feedforward Hodgkin–Huxley neuronal network.

restricted time window, yielding partial synchrony between the corresponding postsynaptic neurons, and then in the next layer downstream, neurons will tend to 'pick-up' synchronous firings in their common inputs and, consequently, they will tend to fire even more synchronously [5]. Finally, we investigate how the alteration of this interlayer link density affects the propagation of the forcing signal towards deeper layers. Based on this mechanism, we determine the minimal density of interlayer links required for an efficient propagation of the weak signal to the deepest layer. We fix the cell size to $S = 6\,\mu m^2$ so that in general Q_i increases with increasing i, and compute Q_{10} for several interlayer link densities above and below 10% over an equal frequency range. We also compute Q_{10} for all-to-all coupling among neurons in neighboring layers. Obtained results are presented in Fig. 4. Evidently, the larger the interlayer link density, the larger the outreach of the forcing signal to the deepest layer. This can be appreciated most clearly for the optimal angular forcing frequency $\omega \approx 0.4$ m/s. Interestingly, however, all curves of Q_{10} for the interlayer link density exceeding 4% are practically identical. This important finding indicates that the synaptic inputs from no more than 4% of neurons in the preceding layer are sufficient for a successful propagation of the signal to the deepest neuronal layer if the forcing frequency is within the sensitive frequency range of individual HH neurons. For finite size feedforward networks with 10 layers, such as considered in this study, if each neuron receives the synaptic inputs from 10% of the neurons in the preceding layer, then neurons in any given layer will share about 1% of the same (common) synaptic inputs [5,22]. Our result suggests that only about 0.4% of the common synaptic inputs in any given layer are enough for an effective propagation of weak rhythmic signals towards deeper layers.

Conclusion

We have shown that the optimal propagation of weak rhythmic signals through feedforward neuronal networks depends significantly on the level of intrinsic noise, the forcing frequency, as well as the density of interlayer links and the coverage of the input introduced to the first layer. Large system sizes, that is, lower levels of intrinsic noise, guarantee a broader range of forcing frequencies that can be effectively amplified by the depth of the feedforward network. Moreover, we have shown that only a rather modest density of interlayer links (4% of all possible) is fully sufficient for an effective propagation of localized stimuli to great depths of the feedforward network. Although this assertion depends on the level of intrinsic noise and the forcing frequency, it indicates that the effectiveness of the amplification mechanism from the input to the output of feedforward networks relies on sparse interlayer connections. In this sense, an overly dense interneuronal communication network between different layers can be considered wasteful.

Acknowledgements

M. Ozer dedicates this article to his mother, Hamide Ozer, who recently passed away. Matjaž Perc acknowledges support from the Slovenian Research Agency (grant Z1-2032).

References

1 Lago-Fernandez LF, Huerta R, Corbacho F, Siguenza JA. Fast response and temporal coding on coherent oscillations in small-world networks. *Phys Rev Lett* 2000; **84**:2758–2761.

2 Yu YG, Liu F, Wang W, Lee TS. Optimal synchrony state for maximal information transmission. *Neuroreport* 2004; **15**:1605–1610.

3 Ozer M, Uzuntarla M, Kayikcioglu T, Graham LJ. Collective temporal coherence for subthreshold signal encoding on a stochastic small-world Hodgkin–Huxley neuronal network. *Phys Lett A* 2008; **372**:6498–6503.

4 Ozer M, Perc M, Uzuntarla M. Stochastic resonance on Newman–Watts networks of Hodgkin–Huxley neurons with local periodic driving. *Phys Lett A* 2009; **373**:964–968.

5 Segev I. Synchrony is stubborn in feedforword cortical networks. *Nat Neurosci* 2003; **6**:543–544.

6 Litvak V, Sompolinsky H, Segev I, Abeles M. On the transmission of rate code in long feedforward networks with excitatory-inhibitory balance. *J Neurosci* 2003; **23**:3006–3015.

7 Middlebrooks JC, Clock AE, Xu L, Green DM. A panoramic code for sound location by cortical neurons. *Science* 1994; **264**:842–844.

8 De Ruyter van Steveninck R, Bialek W. Real-time performance of a movement-sensitive neuron in the blowfly visual system: coding and information transfer in short spike sequences. *Proc R Soc B* 1988; **234**:379–414.

9 Shadlen MN, Newsome WT. The variable discharge of cortical neurons: implications for connectivity, computation, and information coding. *J Neurosci* 1998; **18**:3870–3896.

10 Rossum MCW, Turrigiano GG, Nelson SB. Fast propagation of firing rates through layered networks of neurons. *J Neurosci* 2002; **22**:1956–1966.

11 Abeles M. *Corticonics: neural circuits of the cerebral cortex*. Cambridge: Cambridge University Press; 1991.

12 Reyes AD. Synchrony-dependent propagation of firing rate in iteratively constructed networks in vitro. *Nature Neurosci* 2003; **6**:595–601.

13 Kaplan DT, Clay JR, Manning T, Glass L, Guevara MR, Shrier A. Subthreshold dynamics in periodically stimulated squid giant axons. *Phys Rev Lett* 1996; **76**:4074–4077.

14 Ozer M. Frequency-dependent information coding in neurons with stochastic ion channels for subthreshold periodic forcing. *Phys Lett A* 2006; **354**:258–263.

15 Yu Y, Wang W, Wang JF, Liu F. Resonance-enhanced signal detection and transduction in the Hodgkin-Huxley neuronal systems. *Phys Rev E* 2001; **63**:021907–021912.

16 Wang S, Wang W. Transmission of neural activity in a feedforward network. *NeuroReport* 2005; **16**:807–811.

17 Wang S, Wang W, Liu F. Propagation of firing rate in a feed-forward neuronal network. *Phys Rev Lett* 2006; **96**:018103–018106.

18 Vogels TP, Abbott LF. Signal propagation and logic gating in networks of integrate-and-fire neurons. *J Neurosci* 2005; **25**:10786–10795.

19 Hodgkin AL, Huxley AF. A Quantitative description of membrane current and its application to conduction and exicitation in nerve. *J Physiol* 1952; **117**:500–544.

20 Fox RF. Stochastic versions of the Hodgkin-Huxley equations. *Biophys J* 1997; **72**:2069–2074.

21 Press WH, Teukolsky SA, Vetterling WT, Flannery BP. *Numerical recipes in C*. Cambridge: Cambridge University Press; 1995.

22 Li J, Liu F, Xu D, Wang W. Signal propagation through feedforward neuronal networks with different operational modes. *EPL* 2009; **85**:38006–38011.

23 Perc M, Marhl M. Amplification of information transfer in excitable systems that reside in a steady state near a bifurcation point to complex oscillatory behaviour. *Phys Rev E* 2005; **71**:026229–026236.

24 Hutcheon B, Yarom Y. Resonance, oscillation and the intrinsic frequency preferences of neurons. *Trends Neurosci* 2000; **23**:216–222.

25 Cateau H, Reyes AD. Relation between single neuron and population spiking statistics and effects on network activity. *Phys Rev Lett* 2006; **96**:058101–058104.